

# Increasing-Margin Adversarial (IMA) Training to Improve Adversarial Robustness of Neural Networks

Linhai Ma, Liang Liang

Department of Computer Science,  
University of Miami,  
Coral Gables, FL 33146, USA

**Abstract.** Convolutional neural network (CNN) has surpassed traditional methods for medical image classification. However, CNN is vulnerable to adversarial attacks which may lead to disastrous consequences in medical applications. Although adversarial noises are usually generated by attack algorithms, white-noise-induced adversarial samples can exist, and therefore the threats are real. In this study, we propose a novel training method, named IMA, to improve the robustness of CNN against adversarial noises. During training, the IMA method increases the margins of training samples in the input space, i.e., moving CNN decision boundaries far away from the training samples to improve robustness. The IMA method is evaluated on four publicly available datasets under strong 100-PGD white-box adversarial attacks, and the results show that the proposed method significantly improved CNN classification accuracy on noisy data while keeping a relatively high accuracy on clean data. We hope our approach may facilitate the development of robust applications in medical field.

**Keywords:** Robustness, CNN, Medical image classification.

## 1 Introduction

Convolutional neural network (CNN) has become the first choice for automated medical image analysis due to its superior performance. However, recent studies have shown that they are susceptible to adversarial attacks which add noises to input, and the input perturbation could be imperceptible to human eyes [1]. The threats of adversarial noises to medical image analysis have been revealed by several studies [2]–[5] in previous MICCAI. It is argued that adversarial noises are created by algorithms, not random noises, and may not exist in the real world. However, on the OCT image dataset, we found that ~3% of the noisy samples generated from uniform noise distribution on the noise level of 0.05, can cause ResNet-18 to make wrong classification of OCT images, which suggests that white-noise-induced adversarial samples can exist. For medical applications, ~3% is not a negligible number, and it is clearly worth developing methods to improve CNN adversarial robustness. A general and effective strategy is adversarial training [1], and the basic idea is to add noises to the training samples by using adversarial attacks (e.g. PGD [6]). Through adversarial training, the network can learn from adversarial samples and change decision boundary so that it will become difficult to push the input across the decision boundary by adding a small

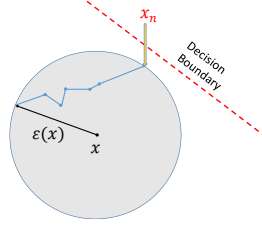


Fig. 1(a). B-PGD (case-0)

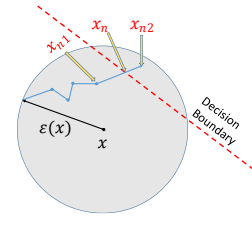


Fig. 1(b). B-PGD (case-1)

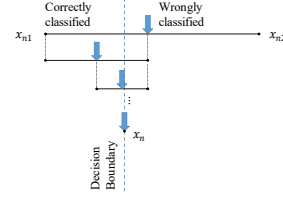


Fig. 2. Binary search

amount of noise. Adversarial training is straightforward but computationally expensive. Thus, one needs to make sure that the generated noisy samples can indeed help to improve robustness: samples with too much noise can harm performance.

We propose a novel method, Increasing-Margin Adversarial (IMA) Training, to improve robustness of deep neural networks for classification tasks. Our method aims to increase margins of training samples (margin is the distance to decision boundary in the input space), i.e., moving decision boundary far away from the training samples to improve robustness. We evaluated our method on four datasets with 100-PGD white-box attack and the results show that our proposed method can achieve a significant improvement in CNN robustness against adversarial noises.

## 2 Methodology

### 2.1 Increasing-Margin Adversarial (IMA) Training

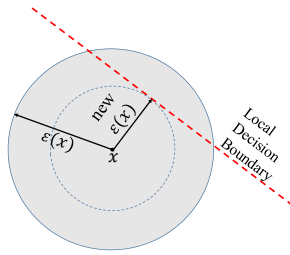


Fig. 3. Shrink Margin

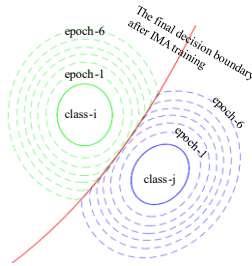


Fig. 4. Equilibrium State

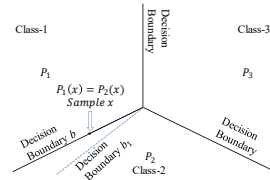


Fig. 5. Three Classes

IMA training process includes two alternating sub-processes: Algorithm 1 to compute IMA loss and update the CNN model, and Algorithm 2 to update margin estimation. In Algorithm 1, by minimizing the IMA loss on clean and noisy samples, the model will try to reach a balance between robustness and accuracy. In Algorithm 2, the sample margins are updated and recorded after each epoch. These estimated margins are used to generate noisy samples for training the model in the next epoch. Our IMA method tries to generate noisy samples on decision boundaries as much as possible:

---

**Algorithm 1** IMA Training to compute loss and update model in one epoch

---

**Input:**  $T = \{(x, y)\}$  is the training set.  $f(x)$  is the model.  $\varepsilon$  is an array containing the estimated margins of individual training samples.  $\beta$  is a coefficient to make a tradeoff between robustness and accuracy on clean data. In a batch,  $X$  contains data samples and  $Y$  contains true class labels.

**Output:** a trained model  $f(x)$  after this epoch

```

1: for Batch  $X, Y$  in  $T$  do
2:   Classify the samples using  $f(x)$  and divide the samples into two groups:
   wrongly-classified  $\{X_0, Y_0\}$  and correctly classified  $\{X_1, Y_1\}$  where  $X =$ 
    $X_0 \cup X_1$ ,  $Y_0 = f(X_0)$  and  $Y_1 = f(X_1)$ 
3:   Run the B-PGD algorithm to get noisy samples  $X_n =$ 
    $PGD(X_1, Y_1, \varepsilon(X_1))$ , and classify these samples:  $Y_n = f(X_n)$ 
4:   Compute the loss  $L$  and its components ( $L_1$ ,  $L_2$  and  $L_3$ ):
5:    $L_1 = \text{Cross-entropy}(Y_0, Y)$ 
6:    $L_2 = \text{Cross-entropy}(Y_1, Y)$ 
7:    $L_3 = \text{Cross-entropy}(Y_n, Y)$ 
8:    $L = (1 - \beta) \times (L_1 + L_2) + \beta \times L_3$ 
9:   Use  $L$  to back-propagate and update the model  $f(x)$ 
10: end for
```

---

adding too much noise to a training sample may significantly reduce accuracy, but adding too little noise may have no effect on improving robustness. We developed Binary-search PGD (B-PGD in Algorithm 3, Fig. 1 and Fig. 2) to find noisy samples on decision boundaries. At the very beginning of the IMA training process, the margins of the training samples are initialized to a small number equal to margin expansion size in Algorithm 2. During IMA training, the margin of a training sample keeps increasing as if a ball is expanding (the ball center is the sample  $x$ , and the radius is the margin  $\varepsilon(x)$ ; it is called  $\varepsilon$ -ball), until the ball of the sample collides with the ball of another sample in a different class. When the two balls collide and therefore a local decision boundary is formed, Algorithm 2 will prevent them from further expansion by shrinking margins (Fig. 3). In the next section, we will show that an equilibrium state (Fig. 4) may exist under which the input margins of the samples are maximized.

## 2.2 The existence of equilibrium

We choose Cross-Entropy loss for classification. We can show that on certain conditions, an equilibrium state (Fig. 4) exists under which the margins of the samples are maximized. To simplify the discussion, we assume there are three classes and three decision boundaries between classes (Fig. 5). The softmax output of the neural network model  $f(x)$  has three components:  $P_1$ ,  $P_2$  and  $P_3$  corresponding to the three classes. If a point (i.e. a data sample)  $x$  is on the decision boundary between Class-1 and Class-2, then  $P_1(x) = P_2(x)$ . The mathematical expectation of the cross-entropy loss of the noisy samples ( $L_3$  in Algorithm 1) in two classes is

$$E = \mathbf{E}_{X_n \in \text{class}_1} \left( -\log(P_1(X_n)) \right) + \mathbf{E}_{X_n \in \text{class}_2} \left( -\log(P_2(X_n)) \right) \quad (1)$$

---

**Algorithm 2** IMA Training to update the margin estimations after each epoch

---

**Input:** training set  $T = \{(x, y)\}$ .  $f(x)$  and  $\varepsilon$  are from Algorithm 1.  $\epsilon_n$  is the noise level.  $\delta$  is the margin expansion step size.  $\|\cdot\|$  denotes the p-norm.

**Output:** updated  $\varepsilon$

```

1: for each sample  $x, y$  in  $T$  do
2:   Classify the samples:  $\hat{y} = f(x)$ 
3:   if  $x$  is wrongly-classified then
4:     Update  $\varepsilon(x) = \delta$  (re-initialize)
5:   else if  $x$  is correctly-classified then
6:     Run the B-PGD algorithm to get the noisy sample  $x_n =$ 
        $PGD(x, y, \varepsilon(x))$ 
7:     if  $x_n$  is on decision boundary (case-1 in Fig. 1(b)) then
8:       Update  $\varepsilon(x) = \|x - x_n\|$  (shrink, Fig. 3)
9:     else (case-0 in Fig. 1(a))
10:      Update  $\varepsilon(x) = \varepsilon(x) + \delta$  (expand)
11:    end if
12:  end if
13: end for
14: Clip  $\varepsilon(x)$  such that it is in the range of  $\delta$  to  $\epsilon_n$ 

```

---

Note: the above process runs in mini-batches. To get better margin estimations, we can run the B-PGD algorithm multiple times.

Given a large noise level  $\epsilon_n$ , the IMA method puts the noisy samples on the decision boundaries. If noisy samples (random variables)  $X_n \in class_1$  and  $X_n \in class_2$  have the same spatial distribution on the decision boundary (denoted by B) between the two classes, then Eq.(1) can be simplified to

$$\begin{aligned}
E &= \mathbf{E}_{X_n \in B} \left( -\log(P_1(X_n)) - \log(P_2(X_n)) \right) = -\mathbf{E}_{X_n \in B} \left( \log(P_1(X_n)P_2(X_n)) \right) \\
&\geq \mathbf{E}_{X_n \in B} \left( -\log \left( \frac{P_1(X_n) + P_2(X_n)}{2} \right)^2 \right)
\end{aligned} \tag{2}$$

E reaches the minimum when  $P_1(X_n) = P_2(X_n)$ .

The analysis shows that the loss of noisy samples will increase if the decision boundaries (i.e. the model  $f(x)$ ) change a little bit from the current state. Thus, when the loss ( $L_1 + L_2$ ) on clean data is minimized and noisy samples are on the decision boundaries, an equilibrium is reached under the assumption that noisy samples have the same spatial distribution on the decision boundaries between classes. This analysis provides the rationale that our IMA method puts the noisy samples on decision boundaries as much as possible, which is significantly different from the theory of the MMA algorithm [7]. If the assumption does not hold, then some oscillations of decision boundaries are expected during training, but the experiment results show that sample margins can still be increased, compared to those trained only on clean data.

---

**Algorithm 3** PGD with Binary-search (B-PGD)

---

**Input:** A training sample  $(x, y)$ .  $f(x)$  and margin  $\varepsilon$ .  $N_{PGD}$  is the number of iterations in PGD.  $N_{Binary}$  is the number of iterations for binary search.

**Output:** noisy sample  $x_n$  for each clean sample  $x$

- 1: Run the standard  $PGD(x, y, \varepsilon(x))$  and obtain a sequence of noisy samples from  $N_{PGD}$  iterations.
  - 2: **if** no adversarial samples are found in the sequence: (case-0 in Fig. 1(a))  
**then**
  - 3:     **return**  $x_n$ , the last sample in the sequence.
  - 4: **else**(case-1 in Fig. 1(b))
  - 5:      $x_{n1}$  and  $x_{n2}$  are two adjacent samples in the sequence.
  - 6:      $x_{n1}$  is the noisy sample that is close to the decision boundary.
  - 7:      $x_{n2}$  is the noisy (adversarial) sample that just goes across the decision boundary the first time.
  - 8:     Run binary search for  $N_{Binary}$  iterations between  $x_{n1}$  and  $x_{n2}$  to find  $x_n$  on the decision boundary (Fig. 2)
  - 9:     **return**  $x_n$
  - 10: **end if**
- 

Note: the above process runs in mini-batches.

### 3 Experiment

We applied the proposed IMA method for four CNNs on four datasets (ECG, Fashion-MNIST, SVHN and OCT) and used 100-PGD to evaluate their robustness. PGD is the strongest first-order white-box attack, and 100 is the number of PGD iterations. To further enhance the attack during model testing, each 100-PGD runs twice. To describe the CNNs, we use "COV (a, b, c, d, e)" to represent a convolution layer with "a" input channels, "b" output channels, kernel size of "c", stride of "d" and padding of "e"; "Linear (f, g)" to denote a linear layer with input size of "f" and output size of "g"; "MP" to denote max-pooling with kernel size of 2; "BN" to denote batch normalization; "LR" to denote leaky ReLU.

To obtain the baseline performance, each CNN was trained with Cross-entropy loss on clean data, which is denoted as "ce". To evaluate the performance, we compare our proposed method with the other four adversarial training methods, including: (1) 20-PGD-based Standard Adversarial Training with noise level  $\epsilon$ , denoted as "adv  $\epsilon$ ", and the loss function is in [8]; (2) Decoupled Direction and Norm Attack [9], denoted as "DDN"; (3) Instance Adaptive Adversarial Training [10], denoted as "IAAT"; (4) adversarial training with TRdeoff-inspired Adversarial DEfense via Surrogate-loss minimization (TRADES) [11], denoted as "TRADE".

#### 3.1 ECG

We used PhysioNet MIT-BIH Arrhythmia ECG Dataset [12] containing 109446 ECG heartbeat records in 5 classes/categories. The dataset has been divided into a training set (87554 samples) and a testing set (21892 samples), which is publicly available.

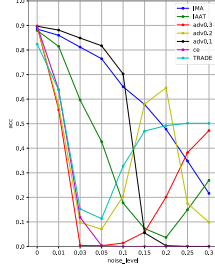


Fig. 6. ECG Linf

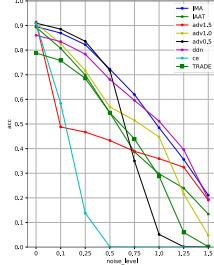


Fig. 7. ECG L2

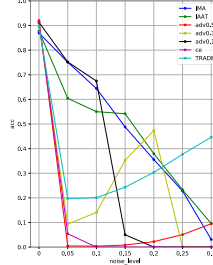


Fig. 8. FM Linf

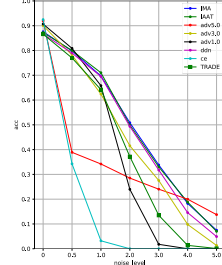


Fig. 9. FM L2

We further divided the training set into a "pure" training set (70043 samples, 80%) and a validation set (17511 samples, 20%). The dataset has a large imbalance between classes, and we performed up-sampling to ensure that there are the same number of samples in each class in the training set. Testing set remains the same. CNN structure for ECG classification is COV(1, 32, 5, 2, 2) -LR-COV(32, 32, 5, 2, 2)-LR-COV(32, 32, 5, 2, 2)-LR-COV(32, 32, 5, 2, 2)-LR-Linear(384, 128)-LR-Linear(128, 128)-LR-Linear(128, 128)-LR-Linear(128, 5). Based on the performance on validation set, we set  $\beta$  to 0.5 in Algorithm 1.  $N_{PGD}$  is 20 for Algorithm 1 and 50 for Algorithm 2.  $N_{Binary}$  is 10.  $\epsilon_n$  is set to the maximum noise level (i.e. 0.3 for L-infinity norm, 1.5 for L2 norm).  $\delta$  is  $\epsilon_n$  divided by the number of epochs. For every method, the number of epochs is 60, optimizer is Adam, and learning rate is 0.001.

To measure robustness on the test set, adversarial noises on different levels (measured by L-infinity or L2 norm) are added. Under L-infinity norm-based attack (Fig. 6), our method "IMA" is better than the compared methods in general, and it can be seen that the model trained by "adv  $\epsilon$ " only behaves well around noise level  $\epsilon$ . "IMA" can keep a high accuracy on clean data (about 90%), while improving the robustness of CNN. Under L2 norm based attack (Fig. 7), our proposed method has the best performance in general.

### 3.2 Fashion-MNIST

We used Fashion-MNIST (FM) dataset. The structure of CNN is COV(1, 32, 3, 1, 1) -LR-MP-COV(32, 64, 3, 1, 1)-LR-MP-Linear( $7 \times 7 \times 64$ , 1024)-LR-Linear(1024, 10). The IMA parameters are the same as those for ECG. Under L-infinity norm based attack (Fig. 8), our proposed method outperformed the compared methods in general. Also, "IMA" can keep a high accuracy on clean data (more than 85%), while improving the robustness of CNN. Under L2 norm based attack (Fig. 9), IMA also has the best performance in general.

### 3.3 SVHN

We used SVHN dataset, and the structure of CNN is COV(3, 32, 3, 1, 1) -BN-ReLU-COV(32, 32, 3, 1, 1)-BN-ReLU-MP-COV(32, 64, 3, 1, 1)-BN-ReLU-COV(64, 64, 3,

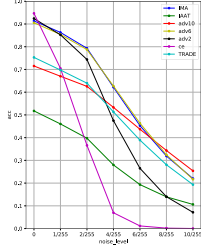


Fig. 10. SVHN Linf

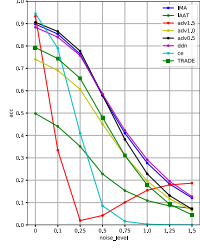


Fig. 11. SVHN L2

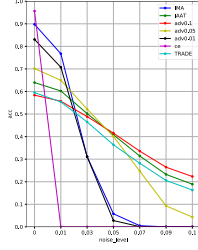


Fig. 12. OCT Linf

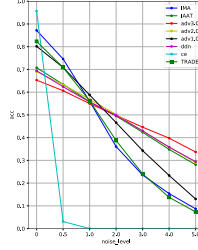


Fig. 13. OCT L2

1, 1)-BN-ReLU-MP-COV(64, 128, 3, 1, 1)-BN-ReLU-COV(128, 128, 3, 1, 1) -BN-ReLU-MP-COV(128, 256, 3, 1, 0)-BN-ReLU-MP-Linear(256, 10). IMA parameters are the same as those for ECG. The results of L-infinity and L2 norm-based attacks are shown in Fig. 10 and Fig. 11, respectively. IMA overperformed the compared methods except for "adv 6" which is as good as IMA. However, to use standard adversarial training "adv  $\epsilon$ ", the user needs to choose the value of  $\epsilon$ , assuming that each data sample has roughly the same margin which may not be true for every dataset. It was lucky that  $\epsilon = 6$  ( $6/255$ ) was chosen in the experiment, and we can see "adv 2" and "adv 10" are not so lucky. IMA can keep a high accuracy in the classification of clean data (more than 90%), while improving the robustness of CNN. Since the margins of the data samples are relatively small, there is no obvious difference between "DDN" and IMA. We note that "DDN" can only handle L2 norm-based attack.

### 3.4 OCT

Retinal optical coherence tomography (OCT) dataset [13] has four classes. Images were resized to  $224 \times 224$ . 1000 samples per class were randomly selected to obtain a training set of 4000 samples. The test set stays unchanged. ResNet-18 with instance normalization was used. To reduce computation cost, we run Algorithm 2 after three training epochs of Algorithm 1. The IMA parameters are similar to those for ECG, except that  $\beta$  is 0.01 in Algorithm 1 and  $\delta$  is  $3 \times \epsilon_n$ /the number of epochs. Optimizer is Adamax for every method. Under L-infinity norm-based attack (Fig. 12), only IMA can keep a high accuracy in the classification of clean data (about 90%), while improving CNN robustness. Under the L2 norm-based attack, IMA has the highest clean accuracy among the defense methods. "adv  $\epsilon$ " is sensitive to the value of  $\epsilon$ , and the underline assumption of every sample having the same margin is not generally true.

## 4 Conclusion

In this study, we proposed a novel Increasing-Margin Adversarial (IMA) Training method to improve the robustness of CNN for classification. Our method aims to increase margin for each of the training samples to improve CNN robustness against adversarial attacks. The experiment results show that our method significantly improved CNN classification accuracy on noisy data while keeping a relatively high

accuracy on clean data. We hope our approach may facilitate the development of robust classification solutions in medical field. We will release the code when the paper is published.

(Note: since the code of MMA [7] was released only a couple of weeks before MICCAI deadline, we do not have sufficient time to read the code and evaluate it.)

## References

1. Akhtar, N. *et al.* Threat of Adversarial Attacks on Deep Learning in Computer Vision: A Survey. *IEEE Access* 6, 14410–14430 (2018).
2. Xue, F.-F. *et al.* Improving Robustness of Medical Image Diagnosis with Denoising Convolutional Neural Networks. in *Medical Image Computing and Computer Assisted Intervention -- MICCAI 2019* (eds. Shen, D. *et al.*) 846–854 (Springer International Publishing, 2019).
3. Huang, Y. *et al.* Some Investigations on Robustness of Deep Learning in Limited Angle Tomography BT - Medical Image Computing and Computer Assisted Intervention – MICCAI 2018. in (eds. Frangi, A. F. *et al.*) 145–153 (Springer International Publishing, 2018).
4. Ozbulak, U. *et al.* Impact of Adversarial Examples on Deep Learning Models for Biomedical Image Segmentation BT - Medical Image Computing and Computer Assisted Intervention – MICCAI 2019. in (eds. Shen, D. *et al.*) 300–308 (Springer International Publishing, 2019).
5. Paschali, M. *et al.* Generalizability vs. Robustness: Investigating Medical Imaging Networks Using Adversarial Examples BT - Medical Image Computing and Computer Assisted Intervention – MICCAI 2018. in (eds. Frangi, A. F. *et al.*) 493–501 (Springer International Publishing, 2018).
6. Madry, A. *et al.* Towards deep learning models resistant to adversarial attacks. *6th Int. Conf. Learn. Represent. ICLR 2018 - Conf. Track Proc.* 1–28 (2018).
7. Ding, G. W. *et al.* Max-Margin Adversarial (MMA) Training: Direct Input Space Margin Maximization through Adversarial Training. 01, 1–34 <http://arxiv.org/abs/1812.02637> (2018).
8. Goodfellow, I. J. *et al.* Explaining and harnessing adversarial examples. *3rd Int. Conf. Learn. Represent. ICLR 2015 - Conf. Track Proc.* 1–11 (2015).
9. Rony, J. *et al.* Decoupling direction and norm for efficient gradient-based l2 adversarial attacks and defenses. *Proc. IEEE Comput. Soc. Conf. Comput. Vis. Pattern Recognit.* 2019-June, 4317–4325 (2019).
10. Balaji, Y. *et al.* Instance adaptive adversarial training: Improved accuracy tradeoffs in neural nets. 1–15 <http://arxiv.org/abs/1910.08051> (2019).
11. Zhang, H. *et al.* Theoretically principled trade-off between robustness and accuracy. *36th Int. Conf. Mach. Learn. ICML 2019* 2019-June, 12907–12929 (2019).
12. Kachuee, M. *et al.* ECG heartbeat classification: A deep transferable representation. *Proc. - 2018 IEEE Int. Conf. Healthc. Informatics, ICHI 2018* 443–444 (2018) doi:10.1109/ICHI.2018.00092.
13. Kermany, D. S. *et al.* Identifying Medical Diagnoses and Treatable Diseases by Image-Based Deep Learning. *Cell* 172, 1122–1131.e9 <https://doi.org/10.1016/j.cell.2018.02.010> (2018).